Nucleic Acids Research, 1992, Vol. 20, No. 23 6159–6166

Recombination of nicked DNA knots by γδ resolvase suggests a variant model for the mechanism of strand exchange

Peter Dröge
Department of Biology, University of Konstanz, PO Box 5560, D-7750 Konstanz, Germany

Received October 29, 1992; Accepted November 10, 1992

ABSTRACT

Fast and efficient recombination catalyzed by γδ resolvase *in vitro* requires negative DNA supercoiling of plasmid substrates. The current model for recombination suggests that supercoiling is required to drive DNA strand exchange within a synaptic complex by 'simple rotation' of DNA-linked resolvase protomers. Surprisingly, DNA knots are recombined efficiently in the absence of supercoiling, whereby the rate of recombination increases with the number of irreducible DNA segment crossings, or nodes, within each substrate knot. Recombination products contain three knot nodes less than substrates, suggesting that a reduction in writhe drives the reaction. However, the proposed protomer rotation model predicts that writhe is not altered during the process of strand transfer but, instead, is reduced only when a synaptic complex disassembles after strand exchange. I present evidence that recombination of knotted and of linear substrates coincides with a disassembly of synaptic complexes. The results lead to a variant model for strand exchange on non-supercoiled substrates in which a specific disassembly of the synaptic complex, triggered by a reduction in writhe, guides the cleaved DNA into the recombinant configuration.

INTRODUCTION

Site-specific DNA recombination plays important roles in various biological systems. These include transposition, bacterial surface and phage tail fiber variation, viral integration and excision, transcription, cell cycle control over plasmid replication, the generation of antibody diversity, and, possibly, an involvement in developmental processes (1–7).

Among these systems are the reactions catalyzed by the resolvases of the bacterial transposons TN3 and γδ. Both systems have been reconstituted *in vitro* with purified recombinases and negatively (–) supercoiled plasmid substrates containing two directly repeated recombination (*res*) sites. Each *res* site, in turn, is composed of three distinct sub-binding sites for resolvase dimers (8). The γδ and TN3 systems are mutually complementary and no energy co-factor is required for fast and efficient recombination in a simple buffer system (9,10). The resolvases belong to a family of closely related site-specific recombinases which includes the DNA invertases (e.g. Hin and Gin), and it is possible that resolvases and invertases employ similar reaction mechanisms (9,11–13).

The wealth of genetic, biochemical, and topological data suggests a multi-step model for the recombination reaction. In a first step, presumably one resolvase dimer binds to each of the three subsites, generating a nucleoprotein complex (resolvosome) on a single *res* site (14). The two resolvosomes can subsequently come together and form a higher order recombinogenic complex which is termed synaptosome (15,16). In a supercoiled substrate, site-synapsis seems to be facilitated by slithering of resolvosomes around an imaginary superhelix axis (17,18).

Topological analyses revealed that three right-handed, plectonemic (–) supercoils are trapped within a synaptosome (9,19–21). In preparation for DNA strand exchange, the two subsites I are paired presumably by the formation of a resolvase tetramer, and the recombinase introduces a staggered double strand cut at the central overlap sequence (Figure 1a,b) (22). Each protomer bound to one half of the crossover region by its C-terminal DNA-binding domain (23) is now, in addition, covalently linked *in cis* to the 5′ end of the cleaved site via its active site residue (16,24,25). Without a rearrangement of DNA-linked protomers, however, DNA cleavage and religation would only restore the parental nucleotide sequence. It is proposed therefore that strand exchange is accompanied by an exchange of protein subunits (9,16,26).

What is the mechanism of strand transfer between subsites I? The current model suggests a 'simple protomer rotation' (16,26), whereby the top two DNA-linked subunits within a resolvase tetramer of D2 (222) symmetry (27,28) are rearranged by a 180° left-handed rotation (Figure 1b to d). Such a rotation of tetrameric subunits leads the cleaved DNA into the recombinant configuration, allows subsequent DNA strand ligation, and exchanges the protein subunits between the two catalytic dimers.

The model of 'simple rotation' is mainly based on three observations. First, more than 95% of the products exhibit the topological structure of a (–) singly-linked catenane (Figure 1e) (29,30). Secondly, the remaining few percent of products show more complex topological structures, such as a 4-noded knot or a figure-8 catenane. It is concluded that these products result from processive left-handed 180° rotations of protomers within the tetramer (31). Thirdly, reactions between two *res* sites differing

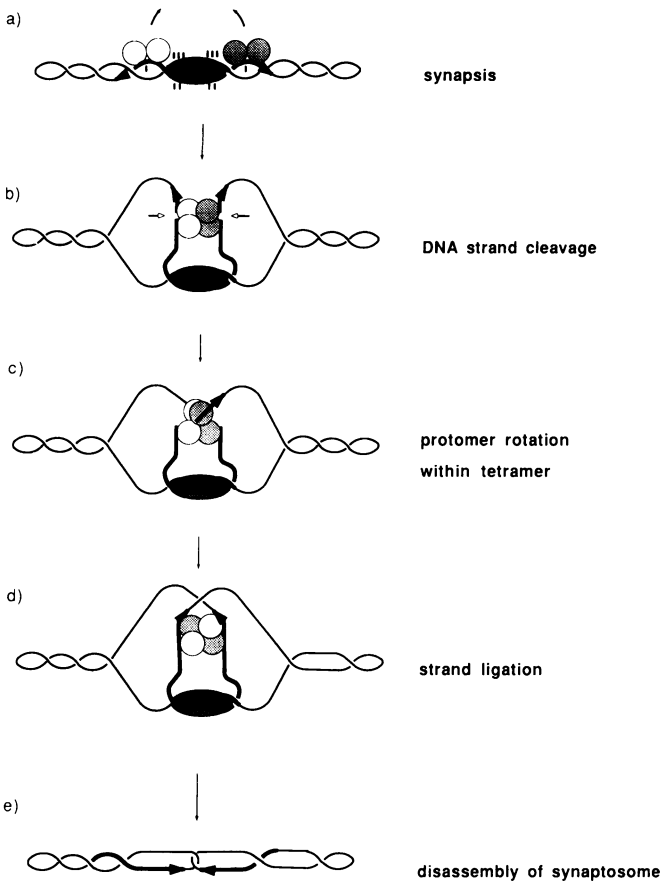

Figure 1. Current model for recombination of (−) supercoiled plasmid DNA. The duplex DNA is represented by a single line, and the substrate for recombination contains 9 plectonemic (−) supercoils. In (a), the two recombination sites (*res*), indicated by arrows in head-to-tail orientation, are paired and synapsis entraps three (−) supercoils. The central part of the synaptosome formed between resolvase and the interwound accessory binding sites II and III of each *res* is highlighted as a shaded oval. In (b), two resolvase dimers (white and filled circles) are bound to subsites I and paired to form a tetramer. Resolvase introduces two staggered double strand cuts at the central dinucleotides of the crossover regions of subsites I (indicated by the arrows in b). If the view is taken from the direction of the accessory binding sites, strand exchange by resolvase subunit exchange is accomplished by a 180° left-handed rotation of the two top protomers within the tetramer (c,d). After strand ligation, the synaptosome disassembles and releases the recombination product, a (−) singly-interlinked catenane (d,e). Note that recombination concomitantly reduces supercoiling so that the catenane product contains 4 (−) supercoils less than the substrate.

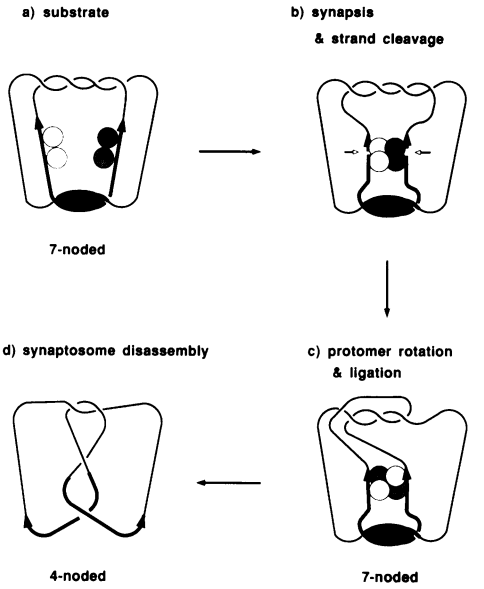

Figure 2. Model for recombination of torus knots by protomer rotation. Schematized as substrate in (a) is a right-handed torus knot, containing 7 (+) nodes (irreducible crossings of DNA segments). The two *res* sites (thick arrows) are in head-to-head orientation, and synapsis traps three (+) nodes, as indicated by the shaded oval (a,b). After the crossover regions of subsites I are aligned by the formation of a tetramer, resolvase introduces two double strand cuts (indicated by the arrows to the left and to the right of the tetramer, respectively, in b). In analogy to Figure 1, strand exchange is accomplished by a 180° left-handed rotation of the two top protomers, followed by ligation (b,c). Note that the movement of DNA segments during protomer rotation does not change the number of nodes in the molecule, nor does it change the quality of nodes because they remain interdomainal. When the synaptosome disassembles after strand exchange is completed, 3 knot nodes are lost due to an unfolding of the molecule. The final product is a 4-noded knot that belongs to the twist family of knots (d).

at one position at the central dinucleotide of subsite I give large amounts of non-recombinant 4-, 6- and 8-noded knots. It is thought that due to the failure to ligate the mismatched sites after the first 180° rotation event, these products result from processive 360° rotations of resolvase subunits within the tetramer (32).

Since no energy co-factor is required for resolution, a key question in this pathway is what provides the energetic drive for the rotation of DNA-linked protomers? The model predicts that the rotation concomitantly increases the twist of the DNA double helix (16,26) which, in turn, reduces (−) supercoiling in domains outside of the synaptosome and is therefore energetically favorable. In agreement with this model is the finding that the rate of recombination is a function of (−) supercoiling of the substrate (33,34), and that the total change in linking number (ΔLk) for the complete reaction is +4 (26,35). This result, in consideration with the presumed geometry of the DNA within the synaptosome, agrees with a total change in twist during strand exchange by +1. Thus, a critical role for (−) supercoiling in this model would be to provide the energy for rotation of DNA-linked protomers.

Recently, we found that (−) supercoiled DNA knots of the torus family, containing *res* sites as inverted repeats, are excellent substrates for TN3 resolvase under standard reaction conditions (21). Since the knots contain *res* sites in inverted orientation, (−) supercoils cannot be trapped within a functional synaptosome (19). Our topological data instead revealed that resolvase forms synaptosomes by trapping three right-handed (+) DNA intertwinings provided by the knot topology (21,36). Thus, in agreement with the current model for recombination as depicted in Figure 1, the topology of (+) torus knots allows the formation of functional synaptosomes while (−) supercoiling provides the energetic drive for the rotation of resolvase protomers during strand transfer.

To gain further insight into the mechanism of strand exchange, I was interested in examining recombination of torus knots that lack (−) supercoiling. As exemplified in Figure 2a with a 7-noded knot, resolvase should form a synaptosome like the one generated on unknotted, supercoiled standard substrates (compare Figure 1b). However, assuming an identical strand exchange mechanism as proposed for standard substrates, no obvious

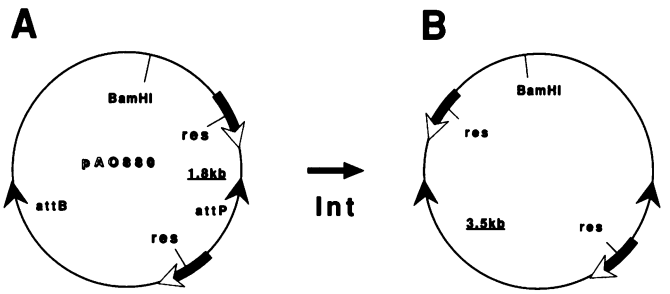

Figure 3. Substrate to generate knotted DNA. (**A**) Only one of the two substrates, pAO880, is illustrated. The 7kb plasmid bears two recombination sites for resolvase (*res*) as direct repeats (arrows with open heads). It also contains two recombination sites, *attP* and *attB* (black arrowheads), for the phage lambda integration system (Int) as inverted repeats. (**B**) Recombination of pAO880 by Int inverts one *res* site with respect to the other so that both are now in head-to-head orientation. This process also changes the relative positions of the sites (for clarity, knotting is omitted in this drawing). The numbers indicate the sizes in kilo-base (kb) pairs of DNA loops generated by synapsis and subsequent BamHI digestion. The second substrate, pAB3, is of identical size and nucleotide sequence as pAO880 but contains the *res* sites diametrically opposed and thus separated by about 3.5kb.

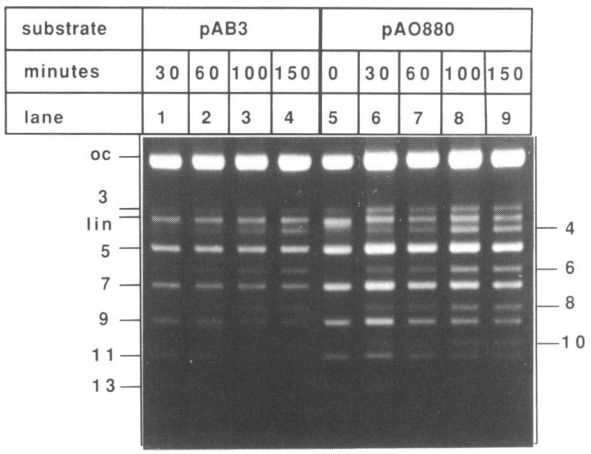

Figure 4. Time course of recombination of nicked knots by γd resolvase. Nicked pAB3 and pAO880 knots were generated, purified, and incubated for various times with resolvase as indicated. Reactions were analyzed by high resolution gel electrophoresis. The substrate knots contain an odd number of nodes (indicated on the left side of the photograph), while product knots contain an even number of nodes (indicated to the right). Lane 5 shows untreated pAO880 knots. lin, Linear; oc, Open circular unknotted DNA.

driving force for protomer rotation exists because the DNA backbone of the knot is nicked. Moreover, the proposed left-handed 180° rotation will change neither the quantity nor the quality of knot nodes, as long as the complex remains stable (Figure 2b,c). Only after strand ligation is completed and the synaptic complex disassembles, three nodes will be lost due to an unfolding of the molecule (Figure 2c,d; see also ref. 21). Thus, an interesting question to investigate is what promotes the exchange reaction if recombination occurs on nicked knots?

MATERIALS AND METHODS

Enzymes and DNA

γδ resolvase was purified as described (37). Phage λ integrase protein (Int) was a gift of H.Echols (University of California, Berkeley). The purification of *E.coli* integration host factor (IHF) has been described (33). Restriction enzymes were purchased from New England Biolabs. Pancreatic DNAse type I was obtained from Cooper Biomedical. pAO880 is a derivative of pAB3 (21).

Reactions

Standard Int reactions contained 20mM Triethanolamine-HCl (pH 7.5), 50mM NaCl, 20mM KCl, 10mM $MgCl_2$, about 25μg DNA per ml, 180ng of Int, 200μg of albumin per ml, and excess IHF in a final volume of 30μl. After 30 min at 25°C, reactions were terminated by heating to 70°C for 10 min. Subsequent nicking reactions contained 300μg ethidiumbromide per ml, and about 100μg per ml DNAseI in Int reaction buffer. After 30 min at 30°C, the reactions were terminated by the addition of SDS, and DNA was extracted with phenol/chloroform and precipitated with ethanol.

Resolvase reactions uniformly contained 20mM Triethanolamine-HCl (pH7.5), 150mM NaCl, 10mM $MgCl_2$, 1mM EDTA, 50μg of DNA per ml, and 10μg resolvase per ml. After incubation at 37°C for the times indicated, reactions were terminated by the addition of SDS to yield a final concentration of 0.5% (w/v).

Analysis of synaptic complex formation

To assay synaptosome formation, 1μg of substrate DNA was incubated with 500ng resolvase at 37°C for the times indicated. Linearization was achieved by addition of BamHI (20 units), and incubation was continued for additional 5 min. Crosslinking was achieved by the addition of glutaraldehyde (Polyscience, Warrington, PA, EM grade) to yield a final concentration of 0.4% and incubation at 15°C for 10 min. The samples were directly loaded onto a 0.8% horizontal agarose gel (89 mM Tris-borate, pH 8.0; 2mM EDTA). At the beginning of the run, the electrophoresis buffer was filled up to a level reaching the upper edges of the gel without covering it. After 10 minutes at 3 V/cm, buffer was added to completely cover the gel, and electrophoresis was continued at 12 V/cm for 4 to 5 hrs at 4°C. DNA was visualized by ethidiumbromide-staining.

High-resolution gel electrophoresis

High-resolution gel electrophoresis of knots was for 24hrs at 1.5V/cm through a 0.8% horizontal agarose gel in a SDS-containing, circulating Tris-acetate buffer (38).

DNA quantification

DNA quantification was achieved by densitometric tracings of photographic negatives of gels stained with ethidiumbromide. The linear response of signal intensities proportional to the amount of DNA present in a single band was assured by analyzing nicked, unknotted pAO880 as a standard. A linear response up to 200ng DNA per band was found with different negatives. This is well within the range of DNA present in any of the substrate or the respective product bands analyzed in the described experiments. To calculate the%-values of recombination, the intensities of substrate and product bands were combined and taken as 100%. From this,% recombination was back evaluated. The data points presented in the plots of Figure 5 are mean-values derived from five and three different experiments using nicked (A) and supercoiled (B) knots, respectively.

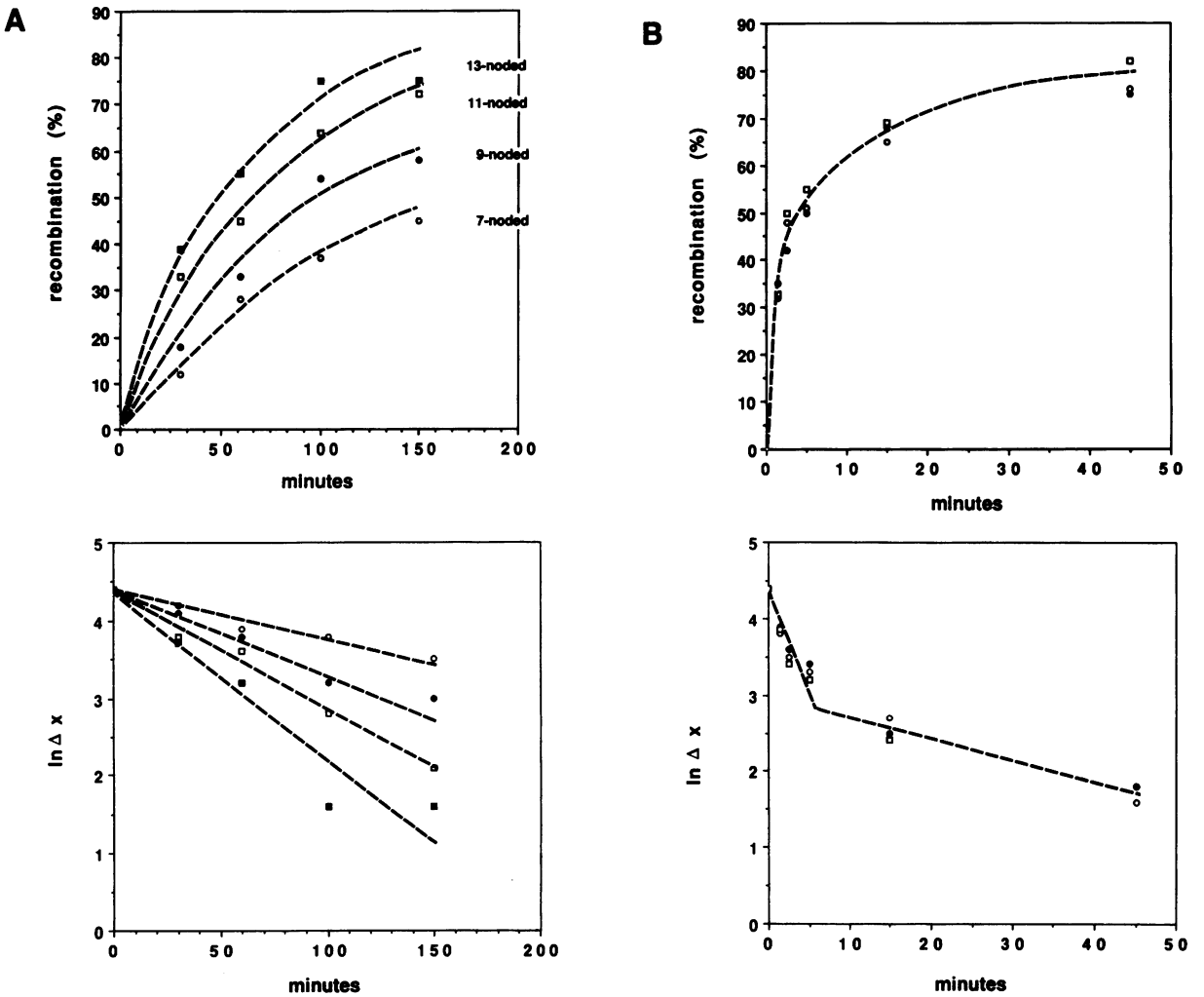

Figure 5. Quantitative analysis of recombination of pAB3 and pAO880 knots. (**A**) Recombination of nicked knots. Densitometric tracings of photographic negatives from five different experiments (3 used pAO880, and 2 used pAB3 as substrate) of the type shown in Figure 4 were analyzed to quantitate recombination. The exceptions are the data points for the 13-noded knot which are derived from 3 experiments using exclusively pAO880 knots. Top panel: 100% recombination was taken as the sum of the intensities of a substrate and the respective product band. From this, the relative recombination efficiency was calculated and the mean-value plotted against incubation time. Bottom panel: Semi-logarithmic plot of the data in the top panel. ΔX is the difference between% recombination at the reaction end point (uniformly taken as 80%) and that at time t. The symbols correspond to those described in the top panel. (**B**) Recombination of supercoiled pAO880 knots. Top panel: Knots were reacted with resolvase for the times indicated. After removal of torsional strain by DNAseI treatment and gel electrophoresis, photographic negatives were analyzed and quantitated as stated above. Each data point represents a mean-value derived from three different experiments. Symbols correspond to the top panel of Figure 5A. Bottom panel: Semi-logarithmic plot of the data presented in the top panel. ΔX is the difference between% recombination at the end point of the reaction (80%) and that at time t.

RESULTS

Recombination rates for nicked DNA knots depend on knot complexity

Two substrates of identical nucleotide sequence and size are tested in this study. Both pAO880 and pAB3 contain two *res* sites as direct repeats, separated by recombination sites *attP* and *attB* for the phage λ integrase system in inverted orientation (Figure 3A). The substrates differ only in the positioning of the *res* sites in their primary sequence, with diametrically opposed sites in pAB3. Supercoiled torus knots of increasing complexity, i.e. with an increasing odd number of nodes, are generated *in vitro* by reacting either (−) supercoiled pAO880 or pAB3 with *E.coli* integration host factor and λ integrase (39,40). A typical integrase reaction yields 50% knotted DNA which contains the *res* sites as inverted repeats (Figure 3B).

We demonstrated previously that incubation of torus knots with resolvase generates products of different complexities and topological structures compared to substrate knots, and that both substrates and products can be separated from each other by high resolution gel electrophoresis (21). Furthermore, it was shown that recombination products obtained from isolated nicked as well as supercoiled pAB3 knots contain three knot nodes less (21). A 7-noded torus knot, for example, is converted into a 4-noded knot of the twist type (Figure 2a,d). Two exceptions are the 5-noded knot, which should be converted into an open circular, unknotted product, and the 3-noded trefoil knot, which, if recombined, should not change its topology (see also ref. 21).

I extended theses studies and investigated whether non-supercoiled knots are recombined by resolvase under standard reaction conditions. An example of such an experiment is presented in Figure 4. By comparison with substrate DNA (lane

5), it is evident that recombination products (with an even number of nodes) are detectable within 30 minutes, and that more complex knots are efficiently recombined during prolonged incubation. The data also reveal that recombination of nicked, unknotted DNA, containing *res* sites as direct repeats, is not detectable under these conditions. If so, singly-interlinked catenanes would have been generated, which migrate between the 3-noded knot and open circular unknotted DNA (21).

It should be noted at this point that, in theory, some of the product knots can also serve as potential substrates for a second recombination event. Thus, a 13-noded torus knot, for example, is converted into a 10-noded twist knot which could be recombined to generate a complicated 7-noded catenane of the twist type as product. This type of catenane would most likely migrate at a position different from that of a torus knot with an equal number of segment crossings (36). However, I found no evidence that second round products are generated.

Figure 5A shows a quantitative analysis derived from 5 different experiments (top panel). Each data point thus represents a mean-value with a maximal standard deviation < 3.5% (recombination). The analysis confirms the notion that the recombination rate increases with knot complexity, and that recombination is efficient even in the absence of (−) supercoiling. From a semi-logarithmic plot of the data (bottom panel), it is also clear that the reactions are relatively slow, with first order rate constants ranging from about 0.006 min^{-1} for the 7-noded knot, to about 0.020 min^{-1} for the 13-noded knot.

It was interesting to compare the kinetics of recombination of nicked knots with those obtained with supercoiled knots. Figure 5B, top panel, shows a quantitative analysis obtained from three different experiments using supercoiled pAO880 knots. Each data point again represents a mean-value with a maximal standard deviation < 2.8% (recombination). The analysis reveals that efficient recombination is fast and occurs within a few minutes of incubation. We noticed before (21) that supercoiled knots are recombined with very similar rates regardless of their complexity. This is confirmed by the present analysis, which shows that recombination rates are about equal for the three knot species tested. Furthermore, reactions on supercoiled knots cannot be fitted to a single exponential (bottom panel), but instead show at least two phases. This is in agreement with an observation made by Castell and Halford in a recent kinetic analysis of recombination by TN21 resolvase (34). In the TN21 system, more than 50% of supercoiled standard substrates are recombined in a fast phase within 5 minutes. This is followed by a slow phase that eventually leads to recombination of close to 100% after several hours. Similarly, with supercoiled torus knots, more than 50% of substrates are recombined within 5 minutes with a rate constant of about 0.3 min^{-1}. This is more than ten times faster than the recombination rate observed for the most complex nicked knot (0.02 min^{-1}).

This biphasic behavior of reactions with supercoiled DNA is not completely understood but might be attributed to the topoisomerase type I activity of resolvase which relaxes (−) supercoiling of a substrate uncoupled from recombination (29,34). Perhaps in the fast phase, resolvase acts on the majority of substrates as a true recombinase. However, in a competing reaction, a substantial fraction of substrates could be topologically relaxed, yielding recombination substrates with significantly lower superhelical densities. These substrates are then recombined at a significantly reduced rate (33,34).

It was surprising to find that recombination of nicked knots is equally efficient as recombination of both supercoiled knots and standard substrates, albeit at a reduced rate. The observation that the recombination rate is a function of knot node density could indicate that a reduction in writhe drives the reaction. However, according to the model presented in Figure 2, strand exchange by left-handed 180° rotation of the top two catalytic protomers does change neither the quantity nor the quality of knot nodes. An alternative 180° right-handed rotation would increase the number of nodes and is, therefore, excluded by the data. If the rotation of subunits within a tetramer is not accompanied by a reduction in writhe, why is recombination a function of knot complexity? One possible explanation is that a step before DNA strand exchange, namely site-synapsis, might be rate-limiting and facilitated on more complex knots.

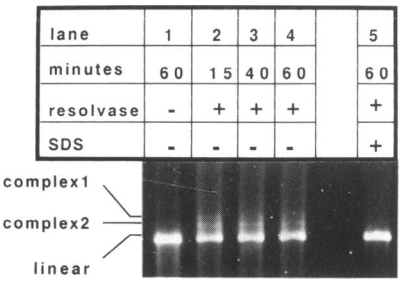

Figure 6. Site-synapsis on knotted and unknotted nicked DNA. A mixture of nicked, knotted (40%) and unknotted (60%) DNA was incubated with (lanes 2 to 5) or without (lane 1) resolvase, followed by BamHI digestion. At the time points indicated, glutaraldehyde was added. After crosslinking, samples were directly loaded onto a horizontal agarose gel. The sample in lane 5 contains SDS, added after crosslinking.

Formation of synaptosomes on nicked knotted and unknotted substrates

The data raise the possibility that synapsis on more complex nicked knots might be facilitated because the molecules contain an increasing number of specific DNA intertwinings suitable for synaptosome formation. I tested site-synapsis by incubating a mixture of nicked substrates containing about 40% knotted and 60% unknotted pAO880 with resolvase, followed by the addition of excess endonuclease BamHI in order to linearize one of the two DNA loops formed upon synapsis. Glutaraldehyde-crosslinking subsequently stabilizes synaptic complexes for further analysis by gel electrophoresis (19).

Within 15 minutes of incubation, two distinct species termed complex 1 and 2 in addition to linearized, uncomplexed DNA are detectable (Figure 6, lane 2). The top band, complex 1, most likely results from synaptic complex formation on knotted DNA and corresponds to a so-called α-structure which contains a DNA loop of about 3.5 kb. Complex 2 also corresponds to an α-structure, but very likely results from synapsis on nicked, unknotted pAO880 generating a smaller DNA loop of only 1.8 kb (compare Figure 3). Control experiments using unknotted substrates bearing *res* sites as direct repeats but at different positions with respect to each other revealed that the difference in electrophoretic mobility is indeed determined by the size of the DNA loop in an α-structure. Furthermore, electron microscopy of complexes formed on nicked pAO880, with and without subsequent linearization, confirmed both specific and efficient pairing of *res* sites (data not shown; ref. 41).

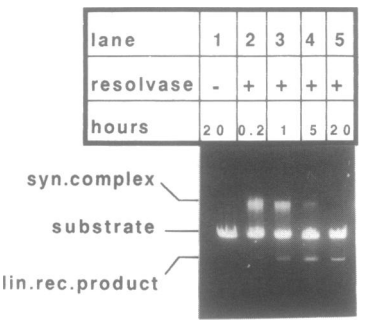

Figure 7. Time course of site-synapsis on and recombination of linearized pAO880. BamHI-linearized pAO880 was incubated with (lanes 2 to 5) or without (lane 1) resolvase for the times indicated. Synapsis and recombination were analyzed on a 0.8% horizontal agarose gel. The 1.8kb circular recombination product was run off the gel. syn complex, Synaptic complex; lin. rec. product, 5.2 kb linear recombination product.

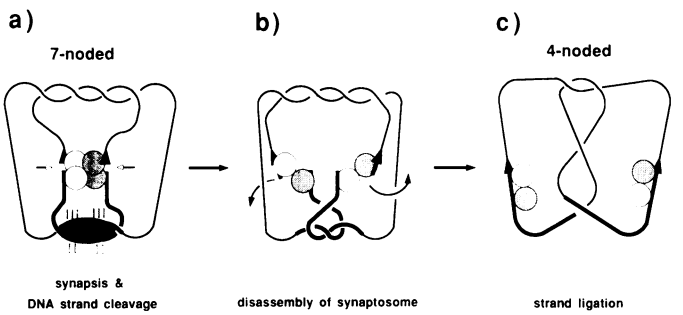

Figure 8. An alternate model for strand exchange. For a detailed description, see Discussion. Starting with a 7-noded knot, synapsis generates a resolvase tetramer which aligns subsites I of both *res*, followed by DNA strand cleavage as indicated by the arrows with open heads (a). The complex resolves and generates two resolvase dimers with exchanged subunits (blank and filled circles). The newly formed dimers, covalently bound to DNA, will lead the four double-stranded ends into the recombinant configuration (a,b). Such a disassembly (the directions of DNA segment movements are indicated by the arrows in (b)) instantaneously reduces the knot node number by 3. Strand ligation is achieved by rearranging protomers within dimers (c).

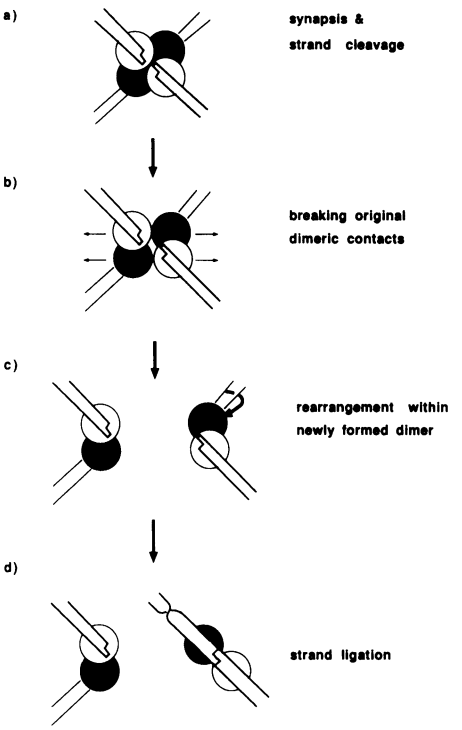

Figure 9. Strand ligation by rearrangement of protomers within dimers. This illustration highlights the disassembly of the tetramer bound to the aligned subsites I. The view is taken down the left arrow in Fig. 8a. After or concomitant with strand cleavage which leads to the covalent attachment of each protomer to a *res* half-site, the tetramer disassembles so that the original dimeric protein-protein contacts are broken (b). Instead, two new dimers are formed and strand alignment and ligation subsequently occurs by rotation of one subunit relative to the other, as exemplified for the newly formed dimer to the right (c,d). Note that such a rotation increases the twist of the DNA at each *res* site by about 0.5.

It is evident from the result in Figure 6 that synapsis on knotted and unknotted substrates occurs within 15 minutes. Furthermore, because synaptosomes are formed on both substrates about equally efficient, synapsis appears not to be facilitated by knot topology. Interestingly, in three different experiments, I found that the amount of both complexes decreases with prolonged incubation time (Figure 6, lanes 2 to 4), indicating that the slow kinetics for recombination seem to coincide with a resolution of synaptosomes.

Recombination of linear substrates coincides with a disassembly of synaptic complexes

The apparent slow disassembly of synaptosomes found with knotted substrates led me to investigate whether sluggish recombination reactions on linear substrates (35,42) are also accompanied by a resolution of synaptic complexes.

Intramolecular recombination between two *res* sites on BamHI-linearized pAO880 should yield a linear 5.2 kb fragment and a 1.8 kb circle. Site-synapsis, however, will result in the formation of an α-structure and, in turn, to a retardation of the 7 kb substrate during electrophoresis. Thus, both recombination and site-synapsis can be monitored simultaneously. As shown in Figure 7, synapsis on linear substrates occurs within 10 minutes (lane 2), but the maximum amount of recombination products is detectable after 1 hr, at a time when the amount of synaptic complexes already decreases (lanes 3 and 4). It seems therefore that intramolecular recombination of linear substrates also coincides with a disassembly of synaptosomes, and it is important to note at this point that a control experiment revealed an identical slow recombination rate when reactions were treated with SDS after crosslinking (not shown). Such a treatment disrupts synaptic complexes and releases recombination products that would otherwise escape detection because they remain trapped within synaptosomes.

DISCUSSION

The main result of this study is that knotted DNA is efficiently recombined by $\gamma\delta$ resolvase in the absence of (−) supercoiling. Compared to supercoiled substrates, however, the rate of recombination is more than 10-fold reduced and a function of knot complexity. In light of the current model for strand exchange, it is puzzling how recombination is influenced by the complexity of knots. First, the DNA backbones of substrates are nicked so that a change in twist during the presumed rotation

of resolvase protomers cannot drive the reaction. Secondly, strand exchange by protein subunit exchange within a tetramer, as depicted in Figure 2, does change neither the quality of knot nodes (they remain interdomainal), nor is the quantity affected as long as the tetramer is stable during the exchange reaction. This stability, however, is an important aspect of the current model for recombination (9,16,32).

One possible explanation for the observed correlation between knot complexity and recombination rate is that site-synapsis is facilitated on more complex knots. Three lines of evidence, however, suggest that different rates for synapsis cannot account for the correlation: First, synapsis on nicked knots is fast and quickly reaches equilibrium compared to the kinetics of recombination. Secondly, compared to synapsis on unknotted substrates, the mere presence of knot nodes obviously does not facilitate synapsis. Thirdly, (−) supercoiling of knots eliminates the effect of knot complexity on recombination rates. Since both supercoiled and nicked knots trap only three (+) right-handed nodes within a functional synaptosome (21), it is conceivable that the rate of site-synapsis is not affected by knot complexity and that (−) supercoiling acts synergistically with knotting in a step after synapsis. A conclusion would be that the rate-limiting step for recombination of nicked knots is after site-synapsis. Interestingly, Parker and Halford (18) came to a similar conclusion for recombination of supercoiled standard substrates. In this case, the rate-limiting step was found to be linked to the DNA strand transfer process.

An alternate model for strand exchange on non-supercoiled substrates involves a specific disassembly of synaptic complexes

The experiments presented in Figures 6 and 7 indicate that slow recombination rates of nicked, knotted and also of linear substrates coincide with a disassembly of synaptosomes. This raises the interesting possibility that DNA strand exchange is functionally linked to a dissociation of synaptosomes. In the following, I present a variant model for the mechanism of strand exchange on nicked knots which could explain recombination as a function of knot complexity.

The variant model is illustrated schematically in Figure 8. In this example, site-synapsis on a 7-noded torus knot aligns the crossover regions, and the four monomers bound to subsites I introduce two double strand breaks (Figure 8a). The monomers are now covalently linked to the *res* half sites *in cis* and concomitant with strand cleavage, the synaptosome, i.e. the complex formed between resolvase and accessory sites II and III, begins to disassemble (Figure 8a,b). The topological structure of the knot now favors specific movements of segments in order to reduce writhe within the DNA molecule. These movements (directions are indicated by the arrows in Figure 8b) disassemble the resolvase tetramer at cleaved subsites I so that two new dimers with exchanged subunits are generated. Furthermore, due to specific protein-protein and protein-DNA linkages, this process leads the DNA ends instantaneously into the recombinant configuration. It is conceivable that this process will be favored with increasing writhe in domains outside of the synaptosome. Alignment of DNA ends and strand ligation is achieved by a rearrangement of protomers within newly formed dimers (Figure 8b,c; see below).

Figure 9 highlights the tetramer bound to the paired crossover regions from a view taken down the left arrow in Figure 8a. After or concomitant with DNA strand cleavage, the original dimeric protein-protein contacts are disrupted (Figure 9a,b), and an alignment of double-stranded ends and religation is achieved by a rearrangement of protomers (Figure 9c,d).

Recombination of supercoiled knots

The data demonstrate that supercoiling of knots eliminates the influence of knot complexity on recombination. In consideration of both the presumed architecture of the synaptosome and the geometry of (−) plectonemic supercoils in domains outside of the synaptic complex, supercoiling could act synergistically with knotting in resolving the tetramer at cleaved subsites I exactly as depicted in Figures 8 and 9, respectively. In fact, supercoiling might become the main driving force for such a disassembly because the supercoil density usually exceeds the knot node density. Supercoiling in addition to knotting would now not only speed up DNA strand transfer, but would also override the influence of knot complexity. Alternatively, supercoiling could change the mechansim of strand transfer and promote exchange via the 'protomer rotation' model. This would also make recombination independent of knot node density.

CONCLUSION

Two functional roles for (−) DNA supercoiling in resolution by $\gamma\delta$ resolvase seem to be firmly established: (i) supercoiling facilitates site-synapsis, and (ii) is involved in the strand transfer reaction. The results of the present study indicate that DNA knotting, instead of supercoiling, can fulfil both roles. First, with substrates bearing inverted *res* sites, knotting allows functional site-synapsis by removal of topological restrictions. Secondly, knotting in the absence of supercoiling seems to promote the strand transfer reaction, whereby a change in writhe (not twist) could drive the reaction. In this case, the 'disassembly model' is an attractive candidate to describe the exchange mechanism. Thus, the actual mechanism of strand exchange might in fact differ and depend on the topological structure of a substrate.

ACKNOWLEDGEMENTS

The main part of this work was performed while on sabbatical at the University of California, Berkeley. I am indebted to N.R.Cozzarelli for his generous support, advice, and encouragement. I wish to thank my colleagues in Berkeley, especially D.E.Adams and R.Kanaar, for their assistance and discussions. Thanks also go to P.Abola for EM analysis of synaptic complex formation. Special thanks go to S.Levene (Dallas) and A.Vologodskii (Moscow) for many helpful discussions. Finally, the support by F.M.Pohl is acknowledged. This work was financed by grants from the National Institutes of Health (GM 31655) and the Deutsche Forschungsgemeinschaft (Dr 187/4-1 and -/4-2) to N.R.C. and P.D., respectively.

REFERENCES

1. Grindley,N.D.F. and Reed,R.R. (1985) *Annu. Rev. Biochem.*, **54**, 863−896.
2. Glasgow,A.G. Hughes,K.T. and Simon,M.I. (1989) *in Mobile DNA* (Berg, D.E. and Howe,M.M., eds) pp. 637−659, American Society of Microbiology, Washington, DC.
3. Weisberg,R. and Landy,A (1983) *in Lambda II* (Hendrix, R.W., Roberts, J.W., Stahl, F.W. and Weisberg, R.A., eds) pp. 211−250, Cold Spring Harbor Laboratory, Cold Spring Harbor, NY.
4. Plasterk,R.H.A. and van de Putte,P. (1984) *Biochim. Biophys. Acta*, **782**, 111−119.
5. Volkert,F.C. and Broach,J.R. (1986) *Cell*, **46**, 541−550.

6. Tonegawa,S. (1983) *Nature*, **302**, 575–581.
7. Matsuoka,M., Nagawa,F., Okazaki,K., Kingsbury,L., Yoshida,K., Müller,U., Larue,D.T., Winer,J.A. and Sakano,H. (1991) *Science*, **254**, 81–86.
8. Grindley,N.D.F., Lauth,M.R., Wells,R.G., Wityk,R.J., Salvo,J.J. and Reed,R.R. (1982) *Cell*, **30**, 19–27.
9. Hatfull,G.F. and Grindley,N.D.F. (1988) *In Genetic Recombination* (Kucherlapati, R. and Smith G.R., eds) pp. 357–396, American Society for Microbiology, Washington, DC.
10. Stark,W.M., Boocock,M.R. and Sherratt,D.J. (1989a) *Trends Genet.*, **5**, 304–309.
11. Kahmann,R., Mertens,G., Klippel,A., Brauer B., Rudt,F. and Koch,C. (1987) The mechanism of G inversion. *In DNA Replication and Recombination*, UCLA Symposia on Molecular and Cellular Biology, New Series, Vol. **47** (McMacken,R. and Kelly,T.J., eds) pp. 681–690.
12. Kanaar,R., Shektman,E., Klippel,A., Dungan,J.M., Kahmann,R. and Cozzarelli,N.R. (1990)*Cell*, **62**, 353–366.
13. Heichman,K.A., Moskowitz,I.P.G. and Johnson,R.C. (1991) *Genes Dev.*, **5**, 1622–1634.
14. Salvo,J.J. and Grindley,N.D.F. (1988a) *EMBO J.*, **7**, 3609–3616.
15. Wasserman,S.A., Dungan,J.M. and Cozzarelli,N.R. (1985) *Science*, **229**, 171–174.
16. Dröge,P., Hatfull,G.F., Grindley,N.D.F. and Cozzarelli,N.R. (1990) *Proc. Natl. Acad. Sci. USA*, **87**, 5336–5340.
17. Benjamin,H.W. and Cozzarelli,N.R. (1986) *Proc. Robert A. Welch Found. Conf. Chem. Res.*, **29**, 107–129.
18. Parker,C.N. and Halford,S.E. (1991) *Cell*, **66**, 781–791.
19. Benjamin,H.W. and Cozzarelli,N.R. (1988) *EMBO J.*, **7**, 1897–1905.
20. Benjamin,H.W. and Cozzarelli,N.R. (1990) *J. Biol. Chem.*, **265**, 6441–6447.
21. Dröge,P. and Cozzarelli,N.R. (1989) *Proc. Natl. Acad. Sci. U.S.A.*, **86**, 6062–6066.
22. Reed,R.R. and Grindley,N.D.F. (1981) *Cell*, **25**, 721–728.
23. Abdel-Meguid,S.S., Grindley,N.D.F., Templeton,N.S. and Steitz,T.A. (1984) *Proc. Natl. Acad. Sci. USA*, **81**, 2001–2005.
24. Reed,R.R. and Moser,C.D. (1984) *Cold Spring Harbor Symp. Quant. Biol.*, **49**, 245–249.
25. Hatfull,G.F. and Grindley,N.D.F. (1986) *Proc. Natl. Acad. Sci.*, **83**, 5429–5433.
26. Stark,W.M., Sherratt,D.J. and Boocock,M.R. (1989b) *Cell*, **58**, 779–790.
27. Sanderson,M.R., Freemont,P.S., Rice,P.R., Goldman,A., Hatfull,G., Grindley,N.D.F. and Steitz,T.A. (1990) *Cell*, **63**, 1323–1329.
28. Hughes,R.E., Hatfull,G.F., Rice,P.A., Steitz,T.A. and Grindley,N.D.F. (1990) *Cell*, **63**, 1331–1338.
29. Krasnow,M.A. and Cozzarelli,N.R. (1983) *Cell*, **32**, 1313–1324.
30. Wasserman,S.A. and Cozzarelli,N..R. (1985) *Proc. Natl. Acad. Sci. USA*, **82**, 1079–1083.
31. Wasserman,S.A. and Cozzarelli,N.R. (1986) *Science*, **232**, 951–960.
32. Stark,W.M., Grindley,N.D.F., Hatfull,G.F. and Boocock,M.R. (1991) *EMBO J.*, 10, 3541–3548.
33. Benjamin,H.W., Matzuk,M.M., Krasnow,M.A. and Cozzarelli,N.R. (1985) *Cell*, **40**, 147–158.
34. Castell,S.E. and Halford,S.E. (1989) *Nucl. Acids Res.*, **17**, 7045–7058.
35. Dungan,J.M. (1988) Ph.D. thesis (Univ. of California, Berkeley).
36. Dröge,P. and Cozzarelli,N.R (1992) *Methods Enzymol.*, **212**, 120–130.
37. Hatfull,G.F., Sanderson,M.R., Freemont,P.S., Raccuia,P.R., Grindley,N.D.F. and Steitz,T.A. (1989) *J. Mol. Biol.*, **208**, 661–667.
38. Sundin,O. and Varshavsky,A. (1981) *Cell*, **25**, 659–669.
39. Spengler,S.J., Stasiak,A. and Cozzarelli,N.R. (1985) *Cell*, **42**, 325–334.
40. Craigie,R. and Mizuuchi,K. (1986) *Cell*, **45**, 793–800.
41. Salvo,J.J. and Grindley,N.D.F. (1988b) *Structure and Expression*, **3**, pp. 105–117, ISBN 0–940030–23–3.
42. Bednarz,A.L., Boocock,M.R. and Sherratt,D.J. (1990) *Genes Dev.*, **4**, 2366–2375.